arXiv:1209.0069v1 [cond-mat.str-el] 1 Sep 2012

# Incomplete devil's staircase in the magnetization curve of $SrCu_2(BO_3)_2$

M. Takigawa,[1, *] M. Horvatić,[2] T. Waki,[3] S. Krämer,[2] C. Berthier,[2]
F. Lévy-Bertrand,[2, †] I. Sheikin,[2] H. Kageyama,[4] Y. Ueda,[1] and F. Mila[5]
[1] *Institute for Solid State Physics, University of Tokyo, Kashiwanoha, Kashiwa, Chiba 277-8581, Japan*
[2] *Laboratoire National des Champs Magnétique Intenses, LNCMI-CNRS (UPR3228), UJF, UPS and INSA, BP 166, 38042 Grenoble Cedex 9, France*
[3] *Department of Materials Science and Engineering, Kyoto University, Kyoto 606-8501, Japan*
[4] *Department of Energy and Hydrocarbon Chemistry, Kyoto University, Kyoto 615-8510, Japan*
[5] *Institute of Theoretical Physics, École Polytechnique Fédérale de Lausanne, CH-1015 Lausanne, Switzerland*

(Dated: September 4, 2012)

We report on NMR and torque measurements on the frustrated quasi-two-dimensional spin-dimer system $SrCu_2(BO_3)_2$ in magnetic fields up to 34 T that reveal a sequence of magnetization plateaus at 1/8, 2/15, 1/6, and 1/4 of the saturation and two incommensurate phases below and above the 1/6 plateau. The magnetic structures determined by NMR involve a stripe order of triplets in all plateaus, suggesting that the incommensurate phases originate from proliferation of domain walls. We propose that the magnetization process of $SrCu_2(BO_3)_2$ is best described as an incomplete devil's staircase.

Coupled-dimer spin systems with singlet ground states have been extensively studied because of a variety of magnetic-field-induced quantum phase transitions. Magnetic fields strong enough to close the zero-field energy gap for the triplet excitations may simultaneously induce a longitudinal magnetization and a transverse antiferromagnetic order, breaking the $U(1)$ rotational symmetry around the field direction. This corresponds to a Bose-Einstein condensation (BEC) of triplets [1]. In the presence of frustration the magnetization curve in higher fields may show plateaus as a consequence of Wigner crystallization of triplet bosons [2].

In studying the magnetization plateaus, the layered compound $SrCu_2(BO_3)_2$ has played a prominent role since the discovery of a sequence of plateaus at 1/8, 1/4 and 1/3 of the saturation value [3]. Its crystal structure consists of two-dimensional layers of orthogonal spin-1/2 dimers in a geometry known as the Shastry-Sutherland lattice [4, 5], in which frustrated interactions drastically reduce the kinetic energy of triplets, leading to the theoretical predictions for plateaus having a superstructure of localized triplets [6, 7]. A symmetry-breaking superstructure of triplets has been indeed observed for $SrCu_2(BO_3)_2$ by Cu and B NMR at the 1/8 plateau [8, 9].

More recent experiments on $SrCu_2(BO_3)_2$ have revealed a rich phase diagram below the 1/4 plateau, but with controversial results. B-NMR [10] and torque [11] measurements have revealed at least two additional phases between the 1/8 and 1/4 plateaus and excluded any plateau with a smaller fraction than 1/8. Other torque measurements, however, have been interpreted as evidence of a sequence of plateaus at 1/9, 1/8, 1/7, 1/6, 1/5, 2/9 and 1/4 [12]. State-of-the-art analytic approaches [13, 14] to determine the effective low-energy triplet Hamiltonian have confirmed the early findings of plateaus at 1/3 and 1/2 [6, 7] and have predicted additional plateaus at 1/9, 2/15, 1/6 and 2/9 according to Ref. [13], and at 1/8, 1/6 and 1/4 according to Ref. [14]. These methods, however, are valid only when the ratio of inter- to intra-dimer couplings is less than 0.5, whereas in $SrCu_2(BO_3)_2$ this ratio is probably around 0.65.

To resolve the discrepancies and to determine the magnetic structures of plateaus, we have carried out torque and $^{11}$B-NMR measurements in static high magnetic fields up to 34 T generated by a 20 MW resistive magnet at LNCMI Grenoble. We observed plateaus at 1/8, 2/15, 1/6, and 1/4 of the saturation and two incommensurate phases below and above the 1/6 plateau. For all plateaus, the magnetic structures determined by high-field NMR involve a stripe order of triplets with different commensurability, suggesting that the incommensurate phases originate from proliferation of domain walls. These findings establish the first observation of an incomplete devil's staircase in quantum antiferromagnets.

To understand the $^{11}$B-NMR spectra, we recall that each boron site generates three NMR lines at the frequencies, $f_k = \gamma(H + H_{\rm int}) + k\nu_Q$, $(k = -1, 0, \text{or } 1)$, where $\nu_Q = 1.25$ MHz is the quadrupole splitting for the external magnetic field $H$ applied along the $c$-axis [15] and $\gamma = 13.66$ MHz/T is the nuclear gyromagnetic ratio. The internal field $H_{\rm int}$ is produced by nearby Cu spins,

$$H_{\rm int} = \sum_i A_i \langle S_c^i \rangle, \tag{1}$$

where $A_i$ is the hyperfine coupling constant to the $i$-th Cu site that has the local magnetization $\langle S_c^i \rangle$ along the $c$-axis. We show in Fig. 1 a part of the low-frequency satellite spectra $(k = -1)$ at $T = 0.43$ K covering the most negative range of internal field ($H_{\rm int} \le -0.13$ T) attributed to those boron sites whose nearest neighbor Cu carries a large magnetization. For this range of $H_{\rm int}$, the low-frequency satellite spectra do not overlap with the central line $(k = 0)$ or high-frequency satellite ($k =$

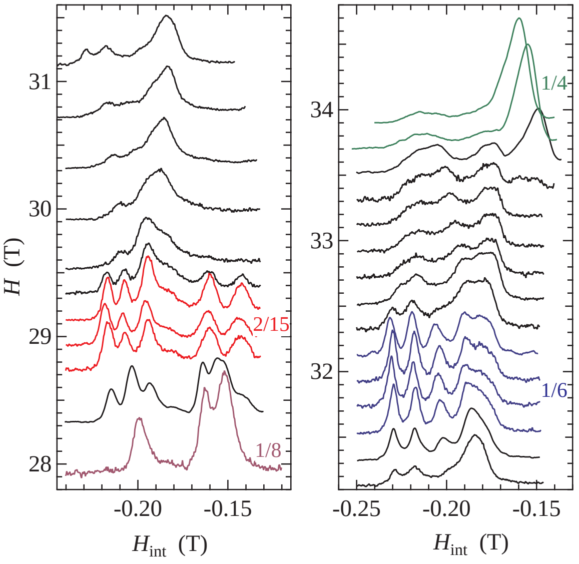

FIG. 1. (color online) A part of the $^{11}$B-NMR spectra covering the most negative range of internal field obtained at $T$ = 0.43 K in various magnetic fields. The values of magnetic fields correspond to the position of the spectral base line on the vertical axis. The purple, red, blue, and green spectra belong to the 1/8, 2/15, 1/6 and 1/4 plateaus, respectively.

1), and therefore they directly give the distribution of $H_{\rm int}$ with typical accuracy of 2 mT.

The spectrum at 27.9 T (purple) belongs to the 1/8 plateau and exhibits sharp peaks that do not move in the entire field range of the plateau, features that are characteristic of a commensurate superstructure. The peak positions agree with previous reports [8–10]. Among the spectra displayed in Fig. 1, we clearly identify two other ranges of field, 28.7 - 29.2 T (red) and 31.5 - 32.2 T (blue), in which the spectra present the same features, suggesting the existence of two additional plateau phases between the 1/8 and 1/4 plateaus. Outside these field ranges, the peaks are rather broad and their positions change continuously with the external field.

The existence of new plateaus is also supported by the magnetization curve shown in Fig. 2 obtained by torque measurement using a cantilever technique. The non-coplanar structure of the $\rm CuBO_3$ layers allows an intradimer Dzyaloshinski-Moriya (DM) interaction, which has been shown to produce a transverse magnetization perpendicular to the magnetic field [16]. The torque ($\tau$) acting on the cantilever then consists of two terms: $\tau = a\mathbf{M}\times\mathbf{H} + b\mathbf{M}\cdot\nabla H$, the first one proportional to the transverse magnetization and the second one to the longitudinal magnetization. Their relative size depends on the precise location and orientation of the sample and of the field profile inside the magnet, which are difficult to know. In the gapped phase of $\rm SrCu_2(BO_3)_2$ below 15 T, where the longitudinal magnetization is strictly zero, $\tau/H$ shown in the inset of Fig. 2 varies linearly with $H$ due to the transverse magnetization. To eliminate this contribution and isolate that of the longitudinal magnetization, we took a linear combination of two measurements of $\tau/H$ taken at different sample positions shown in the inset of Fig. 2, choosing their relative coefficients so that the resulting curve stays zero below 15 T. The result is shown as a black line in the main panel of Fig. 2. It agrees very well with the magnetization determined from the Cu-NMR shift data below 26 T reported in Ref. [8] (open circles).

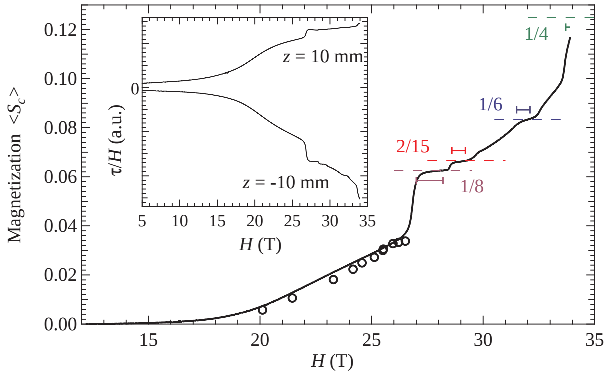

FIG. 2. (color online) Inset: The magnetic-field dependence of the torque divided by field at $T$ = 60 mK for the sample positioned at ±10 mm off the nominal field center. Main panel: The thick black line represents the longitudinal magnetization(see the text) with the vertical scale appropriately adjusted. The magnetization values at 1/8, 2/15, 1/6, and 1/4 of the saturation are shown by the dashed lines. The horizontal bars indicate the field range of the plateaus determined by NMR. The open circles show the magnetization determined from the Cu-NMR shift data from Ref. [8].

The magnetization curve shows a series of plateaus. In addition to the 1/8 plateau and the approach to the 1/4 plateau just outside the available field range, two other plateaus can be clearly recognized: one is adjacent to the 1/8 plateau and the other is approximately half way up to the 1/4 plateau. These field ranges agree perfectly with what we proposed from the field variation of the NMR spectra (the horizontal bars in Fig. 2). The magnetizations of the first three plateaus scale as 1/8 : 2/15 : 1/6, which is partially consistent with the theoretical predictions in Refs. [13] and [14] but does not agree with the values reported in Ref. [12].

Having established the sequence of plateaus, we now discuss the spin structure. The distribution of $H_{\rm int}$ was obtained by an iterative method to deconvolute the quadrupole structure from the NMR spectra [17]. The resulting spectra are displayed in Fig. 3(A) for all plateaus and two intermediate phases above and below the 1/6 plateau. Let us recall that the spin density of one triplet is expected to be distributed primarily over three dimers

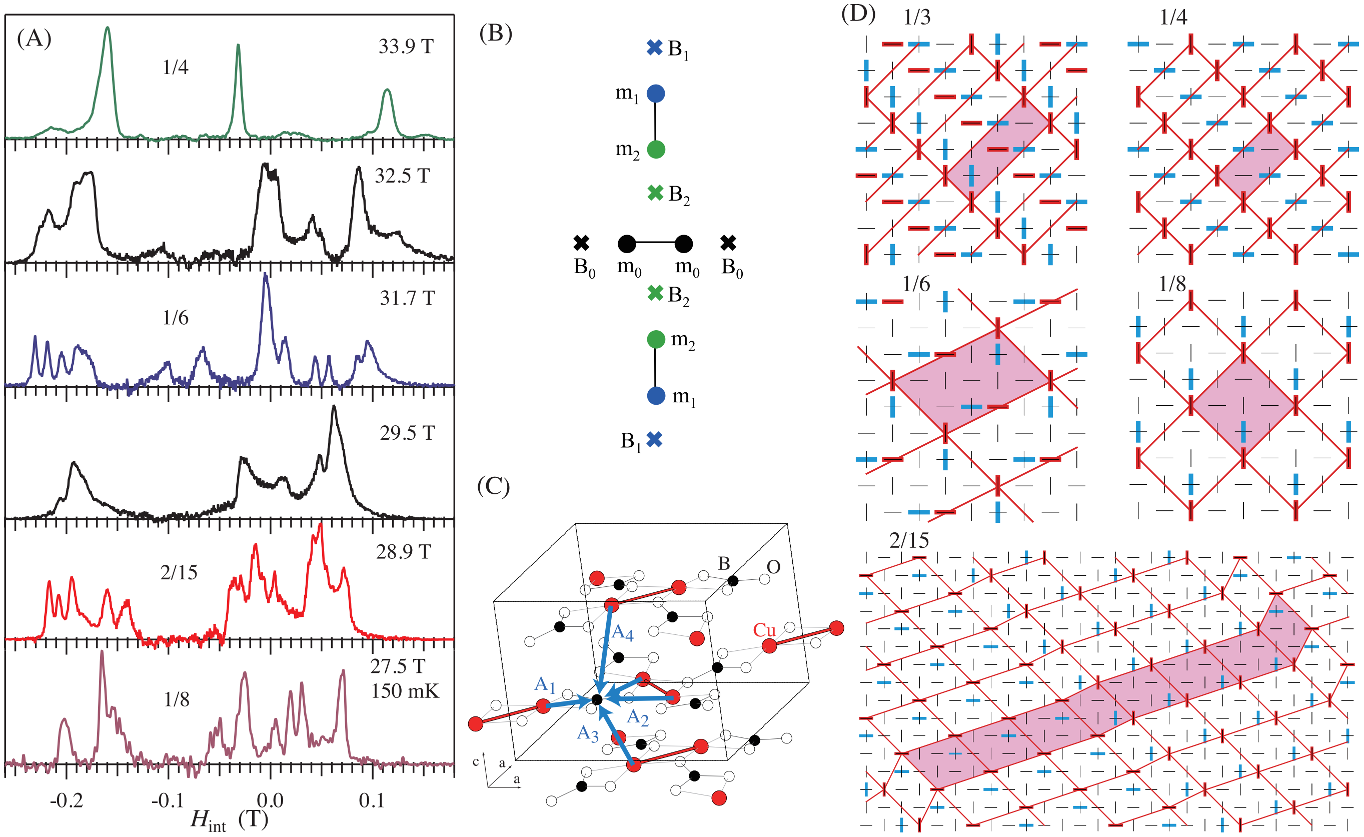

FIG. 3. (color online) (A) Deconvoluted $^{11}$B-NMR spectra representing the distribution of $H_{\rm int}$ obtained at $T = 430$ mK unless explicitly indicated. The data for the 1/8 plateau at 27.5 T was taken from Ref. [9]. (B) An extended triplet and the nearest neighbor B sites. (C) The crystal structure of $\rm SrCu_2(BO_3)_2$. The arrows indicate the hyperfine coupling of a B site to the nearest and the second nearest Cu on the same layer (A1 and A2) as well as the coupling to the third and fourth neighbors on the adjacent layers (A3 and A4). (D) The spin superstructure for the plateau phases. The thin black lines show the lattice of orthogonal Cu-dimers in one layer. The thick red lines show the triplet dimers carrying the largest magnetization $m_0$ in the same layer while the blue lines indicate these triplets on the neighboring layers. The unit cell of each superstructure is shown by the shaded area.

as shown in Fig. 3(B) [8, 18]. The central dimer with a large magnetization $\langle S_c \rangle = m_0 = 0.3 \sim 0.4$ is surrounded by two orthogonal dimers with a negative magnetization $m_2 = -0.1 \sim -0.2$ (antiparallel to the external field) next to the central dimer and a positive magnetization $m_1 = 0.2 \sim 0.3$ at the ends. We call this cluster an *extended triplet*. It is stabilized by the cooperative (non frustrated) action of the polarized spins of the central triplet on the two neighboring dimers, and by its strongly reduced coupling to surrounding spins due to frustration. Other dimers have much smaller magnetization. We define $\rm B_0$, $\rm B_1$, and $\rm B_2$ as the B sites nearest to $m_0$, $m_1$, and $m_2$, respectively. All plateau spectra show a group of lines near $H_{\rm int} = -0.2$ T isolated from other lines (the part shown in Fig. 1), which comes from $\rm B_0$ and $\rm B_1$ sites. The magnetic structures of plateaus were determined as follows:

(1) The coupling constant $A_i$ is the sum of the short-ranged transferred hyperfine coupling and the classical dipolar coupling. The coupling to the nearest neighbor Cu spin (see Fig. 3(C)) is by far the largest. The second neighbor gives a very small contribution due to the cancellation between the transferred and dipolar terms, and it is much smaller than the dipolar coupling to the third and fourth neighbors. Therefore, to zeroth order, $H_{\rm int}$ is simply proportional to the magnetization on the nearest neighbor Cu site.

(2) The zeroth-order NMR lines then shift and may be split by the dipolar field from the third and fourth neighbors, which are on the adjacent layers as shown in Fig. 3(C). This means that the spectral features, which distinguish one plateau from the others, are primarily due to the interlayer stacking of extended triplets rather than the in-plane spin configuration. We found that the partial spectrum of $\rm B_0$ and $\rm B_1$ sites is specific enough in all cases to select a unique in-plane structure allowing at least one stacking pattern qualitatively consistent with the observed spectrum. Figure 3(D) shows the structures thus determined, including the one for the 1/3 plateau which we found by applying the same analysis to the

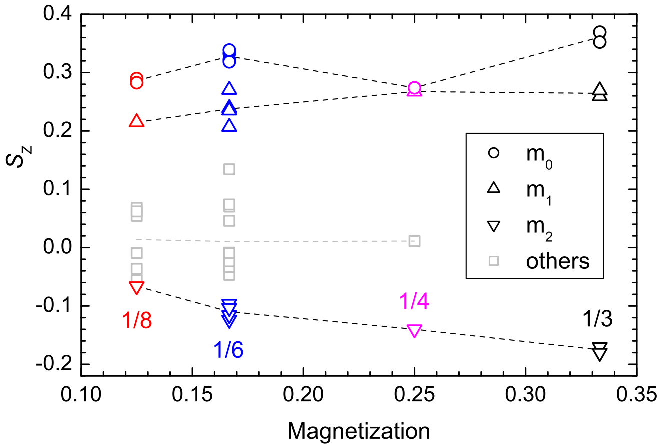

FIG. 4. (color online) Distribution of local magnetization in the 1/8, 1/6, 1/4 and 1/3 plateau phases deduced from the peak positions of the B-NMR spectra.

spectrum reported by Stern *et al.* [19]. The unit cell of all these structures involve two layers as in the crystal structure.

(3) As a consistency check, we have tried to account for the entire spectrum of the 1/8, 1/6, 1/4, and 1/3 plateaus assuming the structure shown in Fig. 3(D). For these structures, we were able to assign a particular peak value of $H_{\rm int}$ to each B site almost uniquely. The values of the local magnetization $\langle S_c^i \rangle$ have then been determined by solving Eq. (1), since there is an equal number of inequivalent Cu and B sites in a unit cell of the superlattice (see the Supplemental Material [20]). The resulting values of $m_0$, $m_1$, and $m_2$, displayed in Fig. 4, change very little from one plateau to the next, as expected.

All plateaus show stripe order of triplets as shown in Fig. 3(D). The structures for the 1/3 plateau and the 1/4 plateau agree with the theoretical prediction [6, 7] The former structure is a simple close packing of extended triplets, while in the other structures they are progressively more spaced by sites having much smaller polarization. The structure of the 1/6 plateau can be obtained from that of the 1/3 plateau by removing every other triplet from each stripe. Similarly, the square unit cell of the 1/8 plateau is obtained by removing every other triplet from each stripe of the 1/4 plateau. Note that this structure of the 1/8 plateau is different from the one with a rhomboid unit cell, which was proposed based on the previous Cu-NMR experiments [8] (see Supplemental Material [20]). Finally, the structure of the 2/15 plateau consists of alternating domains of 1/8 and 1/6 structures. More precisely, three stripes of the 1/8 rhomboid structure are followed by a single stripe of the 1/6 structure. This is a good example showing how the proliferation of domain walls leads to a structure of higher order commensurability. We should remark that the structures of the 1/6 and 2/15 plateaus are not the ones predicted theoretically[13], presumably because the ratio of inter- to intradimer coupling is significantly larger than 0.5.

Let us now discuss the spectra in the intermediate phases below and above the 1/6 plateau. As shown in Fig. 3(A), they share a common feature to the spectra in the plateaus, that is the $B_0$ and $B_1$ lines at large negative values of $H_{\rm int} \sim -0.2$ T well separated from the rest of the spectra. This indicates that the fully polarized extended triplets remain immobile at least within the time scale of NMR measurement (around 100 $\mu$s), i.e. they are completely localized. However, unlike in the plateaus, the spectra in the intermediate phases consist of a few broad continuous lines, which cannot be decomposed into discrete narrow lines. Such a spectral feature indicates an incommensurate magnetic structure. This is quite natural since the density of triplets, i.e. the magnetization, changes continuously, and therefore generally takes irrational values. Intermediate phases could have a commensurate structure if the system separates into two commensurate phases with their volume ratio changing with field, or if a commensurate fraction of triplets forming a superstructure coexists with the rest of delocalized triplets. However, the NMR spectra in such cases should have sharp peaks similar to the spectra in the plateau phases, clearly inconsistent with the experimental observation.

As an attempt to put the results in a broader perspective, we conjecture that the sequence of phases revealed by the present measurements is the first example of an *incomplete devil's staircase* in the context of the magnetization curve of a quantum antiferromagnet. The concept was introduced in the investigation of commensurate-incommensurate transitions: a devil's staircase is an infinite sequence of commensurate phases with increasingly large commensurability built by the proliferation of domain walls between domains of different commensurability [21]. It becomes *incomplete* when the infinite sequences of high commensurability phases with small steps are replaced by incommensurate phases [22].

This interpretation is supported not only by the sequence of fractional magnetization ratios in $SrCu_2(BO_3)_2$, which is typical of a devil's staircase [21], but also by the stripe structure of the plateaus determined by the present NMR experiments, which naturally allows the formation of domain walls, as seems to be the case in the 2/15 plateau. It would be very interesting to check this interpretation by a direct measurement of the wave-vector of the structure, which has become accessible for the required magnetic field range by neutron scattering performed in pulsed field [23]. Finally, we note that it remains a challenge for theory to explain why higher commensurability plateaus (or even lower ones such as 1/7) are unstable towards the formation of incommensurate phases.

We thank Julien Dorier, Katsuaki Kodama, Kai Schmidt and Raivo Stern for valuable discussions. This work was supported partly by a Grant-in-Aid for Scientific Research (No. 21340093) from JSPS, by a GCOE program from MEXT Japan, by French ANR project NEMSICOM, by European Commission through the EuroMagNET network (Contract No. 228043), by the Swiss National Fund, and by MaNEP. FM acknowledges the hospitality of ISSP.

---

[*] masashi@issp.u-tokyo.ac.jp

[†] Present address: Institut Néel, CNRS and UFJ, BP 166, 38042 Grenoble Cedex 9, France

[1] T. Giamarchi, C. Rüegg, O. Tchernyshyov, Nat. Phys. **4**, 198 (2008).

[2] M. Takigawa and F. Mila, Introduction to Frustrated Magnetism, Eds. C. Lacroix, P. Mendels, F. Mila, Springer, p. 241 (2011).

[3] K. Onizuka, H. Kageyama, Y. Narumi, K. Kindo, Y. Ueda, T. Goto, J. Phys. Soc. Jpn. **69**, 1016 (2000).

[4] B. S. Shastry and B. Sutherland, Physica **108B** 1308 (1981).

[5] H. Kageyama, K.Yoshimura, R. Stern, N.V. Mushnikov, K. Onizuka, M. Kato, K. Kosuge, C.P. Slichter, T. Goto and Y. Ueda, Phys. Rev. Lett. **82**, 3168 (1999).

[6] S. Miyahara and K. Ueda, Phys. Rev. B **61**, 3417 (2000).

[7] T. Momoi and K. Totsuka, Phys. Rev. B **62**, 15067 (2000).

[8] K. Kodama, M. Takigawa, M. Horvatić, C. Berthier, H. Kageyama, Y. Ueda, S. Miyahara, F. Becca and F. Mila, Science **298**, 395 (2002).

[9] K. Kodama, M. Takigawa, M. Horvatić, C. Berthier, H. Kageyama, Y. Ueda, S. Miyahara, F. Becca and F. Mila, Physica B **346-347**, 27 (2004).

[10] M. Takigawa, S. Matsubara, M. Horvatić, C. Berthier, H. Kageyama and Y. Ueda, Phys. Rev. Lett. **101**, 037202 (2008).

[11] F. Levy, I. Sheikin, C. Berthier, M. Horvatić, M. Takigawa, H. Kageyama, T. Waki and Y. Ueda, EPL **81**, 67004 (2008).

[12] S. E. Sebastian, N. Harrison, P. Sengupta, C. D. Batista, S. Francoual, E. Palm, T. Murphy, N. Marcano, H. A. Dabkowska, and B. D. Gaulin, PNAS **105**, 20157 (2008).

[13] J. Dorier, K. P. Schmidt, and F. Mila, Phys. Rev. Lett. **101**, 250402 (2008).

[14] A. Abendschein and S. Capponi, Phys. Rev. Lett. **101**, 227201 (2008).

[15] K. Kodama, J. Yamazaki, M. Takigawa, H. Kageyama, K. Onizuka and Y. Ueda, J. Phys.: Condens Matter **14** L319 (2002).

[16] S. Miyahara, J.-B. Fouet, S. R. Manmana, R. M. Noack, H. Mayaffre, I. Sheikin, C. Berthier and F. Mila, *et al.*, Phys. Rev. B **75**, 184402 (2007).

[17] F. Mila *et al.*, unpublished.

[18] S. Miyahara, F. Becca and F. Mila: Phys. Rev. B **68**, 024401 (2003).

[19] R. Stern, I. Heinmaa, P.L. Kuhns, A.P. Reyes, W.G. Moulton, H.A. Dabkowska and B.D. Gaulin, NHMFL Research Report (2004) No. 278.

[20] See Supplemental Materials at (URL) for detailed procedure to obtain the local magnetization by fitting the experimental spectra.

[21] P. Bak, Rep. Prog. Phys. **45**, 587 (1982).

[22] S. Aubry, Solitons and Condensed Matter Physics ed A R Bishop and T Schneider (Berlin: Springer-Verlag), p. 264 (1979).

[23] M. Matsuda, K. Ohoyama, S. Yoshii, H. Nojiri, P. Frings, F. Duc, B. Vignolle, G. L. J. A. Rikken, L.-P. Regnault, S.-H. Lee, H. Ueda and Y. Ueda *et al.*, Phys. Rev. Lett. **104**, 047201 (2010).